Supporting Information

Water-soluble bright NIR AIEgens with hybrid ROS for wash-free mitochondrial "off-on" imaging and photodynamic therapy

Fang-Zhou Xu [a], Cheng-Yun Wang *[a], Qi Wang [a], Jian-Wei Zou [b], Yi-Jie Qiao [a], Zhi-Qian Guo [a] Weijun Zhao*[a] and Wei-Hong Zhu*[a]

[a] Key Laboratory for Advanced Materials and Institute of Fine Chemicals, School of Chemistry and Molecular Engineering, East China University of Science and Technology, 130 Meilong Road, Shanghai 200237, PR China. E-mail: cywang@ecust.edu.cn; zhwj@ecust.edu.cn; whzhu@ecust.edu.cn

[b] NingboTech University, Ningbo 315100, Zhejiang, PR China.

Table of Contents

Materials and methods

All chemicals were commercially purchased and used without further purification. The ^{1}H and ^{13}C NMR spectra were recorded with a Bruker AM 400 spectrometer or an Ascend 600 spectrometer, using TMS as an internal standard. High resolution mass spectra were recorded with a Waters LCT Premier XE spectrometer. UV-vis and fluorescence spectra were recorded with an Agilent Cary 60 spectrophotometer and F97pro fluorescence spectrophotometer respectively. Cell images were recorded with a Nikon A1R laser scanning confocal microscopy. EPR spectra were recorded with a Brucker EMX-8/2.7 electro-spin resonance spectrometer.

Synthesis of TEPP, TTPP, CEPP, CTPP and MTPP

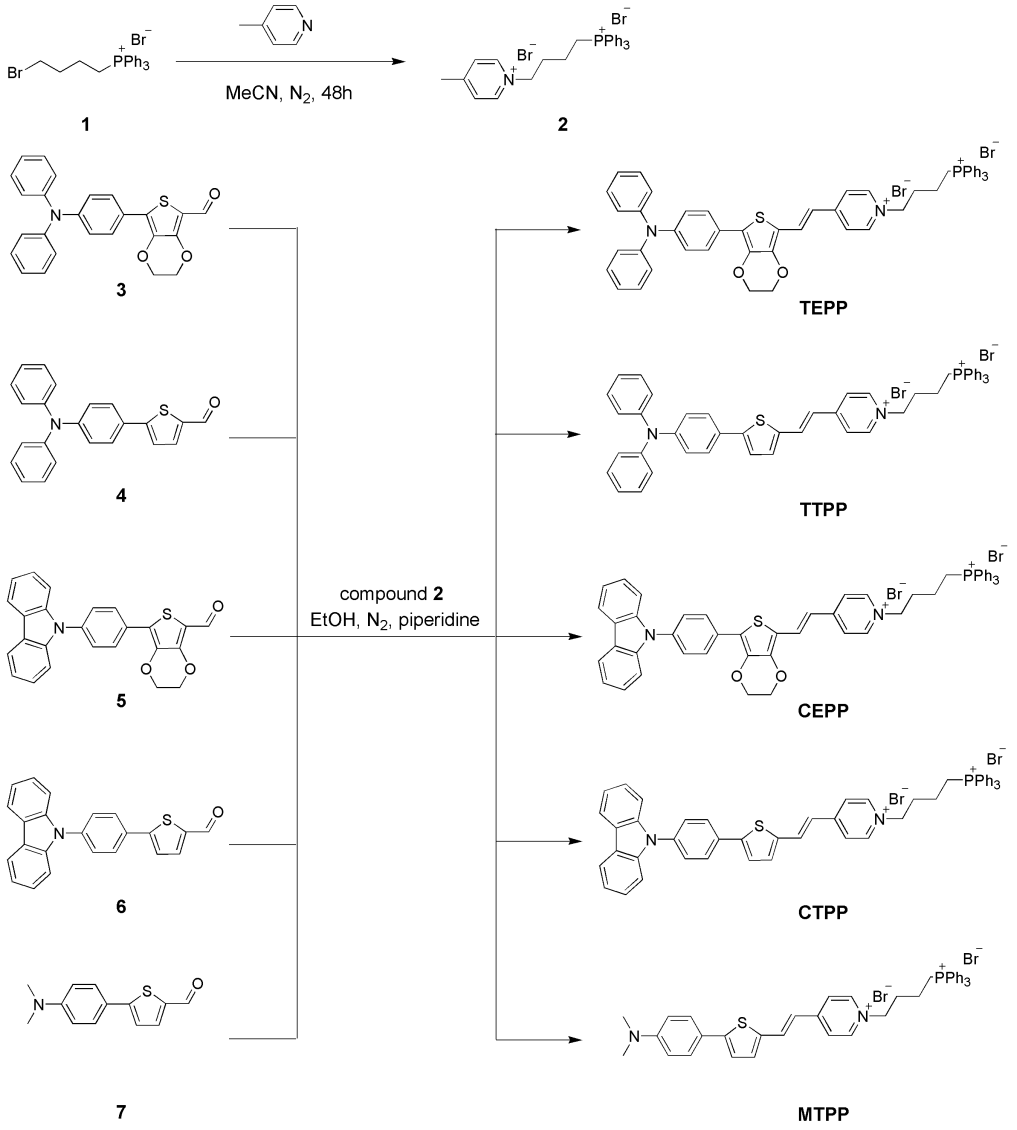

Scheme S1 Synthetic routes of **TEPP**, **TTPP**, **CEPP**, **CTPP** and **MTPP**.

Compound **1** and **3-7** were prepared according to reported literatures.[1]

Synthesis of compound 2. A solution of compound 1 (1.91 g, 4.0 mmol) and 4-picoline (0.56 g, 8.0 mmol) in acetonitrile (40 mL) was refluxed under nitrogen for 48 h. After cooling to room temperature, the solvent was removed by evaporation under reduced pressure and then dissolved in minimal amount of methanol. The methanol solution was dropped into ether (80 mL) to yield a pale pink precipitate. After decantation, the precipitate was carefully washed with ethyl acetate (30 mL × 3) to afford a white solid (2.08 g, 91% of yield). ^{1}H NMR (400 MHz, DMSO-d_6, ppm): δ 8.94 (d, J = 6.8 Hz, 2 H), 7.98 (d, J = 6.0 Hz, 2 H), 7.92 (td, J = 7.2, 2.4 Hz, 3 H), 7.85–7.75 (m, 12 H), 4.61 (t, J = 7.2 Hz, 2 H), 3.72 (td, J = 15, 2.0 Hz, 2 H), 2.61 (s, 3 H), 2.15–2.08 (m, 2 H), 1.58–1.48 (m, 2H). ^{13}C NMR (100 MHz, $CDCl_3$, ppm): δ 158.27, 144.94, 135.21, 135.18, 133.80, 133.70, 130.72, 130.60, 128.39, 118.26, 117.41. 58.75, 32.47, 32.30, 22.61, 22.25, 22.09, 19.39, 19.36. Mass spectrometry (ESI-MS, m/z): $[M–HBr–Br]^+$ calcd. for $C_{28}H_{29}NP^+$: 410.2027; found: 410.2047.

Synthesis of TEPP, TTPP, CEPP, CTPP and MTPP. Taking **TEPP** as an example, the synthetic steps of other AIEgens are similar. A solution of compound 2 (192 mg, 0.35 mmol), compound 3 (83 mg, 0.20 mmol) and Na_2SO_4 (100 mg) in ethanol (10 mL) was refluxed under nitrogen and catalyzed by a few drops of piperidine overnight. After cooling to room temperature, the solvent was removed by evaporation under reduced pressure. The residue was purified with a neutral aluminum oxide column using a DCM and methanol mixture (30 : 1 v/v) as the eluting solvent to afford a purplish red powder of **TEPP**.

TEPP ^{1}H NMR (400 MHz, CD_3OD, ppm): δ 8.60 (d, J = 7.2 Hz, 2 H), 7.95–7.87 (m, 6 H), 7.85–7.74 (m, 12 H), 7.64 (d, J = 8.8 Hz, 2 H), 7.29 (t, J = 7.6 Hz, 4 H), 7.09–7.06 (m, 6 H), 6.98 (d, J = 8.8 Hz, 2 H), 6.93 (d, J = 15.6 Hz, d, 1 H), 4.49 (t, J = 7.6 Hz, 2 H), 4.45–4.37 (m, 4 H), 3.56 (td, J = 15.0, 2.8 Hz, 2 H), 2.27–2.20 (m, 2 H), 1.80–1.70 (m, 2 H). ^{13}C NMR (150 MHz, CD_3OD, ppm): δ 154.17, 147.78, 147.16, 145.34, 143.10, 135.01, 133.56, 133.49, 130.29, 130.20, 129.21, 127.11, 124.74, 123.50, 122.44, 121.99, 112.38, 65.23, 64.64, 58.59, 31.51, 31.39, 21.21, 20.86, 19.03, 19.01. Mass spectrometry (ESI-MS, m/z): $[M–2Br]^{2+}$ calcd. for $C_{53}H_{47}N_2O_2PS^{2+}$: 403.1543; found: 403.1531.

TTPP ^{1}H NMR (400 MHz, CD_3OD, ppm): δ 8.67 (d, J = 6.8 Hz, 2 H), 8.11 (d, J = 15.6 Hz, 1 H), 8.04 (d, J = 6.8 Hz, 2 H), 7.90 (td, J = 7.2, 2.0 Hz, 3 H), 7.85–7.74 (m, 12 H), 7.59 (d, J = 8.8 Hz, 2 H), 7.48 (d, J = 4.0 Hz, 1 H), 7.39 (d, J = 4.0 Hz, 1 H), 7.31 (t, J = 8.0 Hz, 4 H), 7.11–7.02 (m, 9 H), 4.52 (t, J = 7.4 Hz, 2 H), 3.54 (td, J = 14.8, 2.8 Hz, 2 H), 2.28–2.21 (m, 2 H), 1.81–1.73 (m, 2 H). ^{13}C NMR (150 MHz, CD_3OD, ppm): δ 154.01, 149.11, 148.61, 147.15, 143.50, 138.77, 135.02, 134.93, 134.15, 133.55, 133.49, 130.29, 130.21, 129.24, 126.54, 124.82, 124.21, 123.59, 123.46, 123.17, 122.24, 120.14, 118.49, 117.92, 58.88, 31.54, 31.42, 21.20, 20.85, 19.04, 19.02. Mass spectrometry (ESI-MS, m/z): $[M–2Br]^{2+}$ calcd. for $C_{51}H_{45}N_2PS^{2+}$: 374.1515; found: 374.1570.

CEPP ^{1}H NMR (400 MHz, CD_3OD, ppm): δ 8.54 (d, J = 6.8 Hz, 2 H), 8.13 (d, J = 7.7 Hz, 2 H), 8.04 (d, J = 8.6 Hz, 2 H), 7.92–7.88 (m, 3 H), 7.85–7.81 (m, 6 H), 7.79–7.74 (m, 9 H), 7.61 (d, J = 8.6 Hz, 2 H), 7.47–7.38 (m, 4 H), 7.27 (t, J = 7.3 Hz, 2 H), 6.96 (d, J = 15.8 Hz, 1 H), 4.51–4.44 (m, 6 H), 3.52 (td, J = 15.2, 2.4 Hz, 2 H), 2.23–2.16 (m, 2 H), 1.80–1.68 (m, 2 H). ^{13}C NMR (150 MHz, CD_3OD, ppm): δ 153.60, 144.82, 142.91, 140.12, 139.21, 136.66, 135.00, 133.47, 130.88, 130.21, 127.39, 126.39, 125.95, 123.39, 122.44, 121.08, 120.14, 119.99, 118.66, 118.44, 117.87, 113.56, 109.51, 65.18, 64.80, 58.62, 31.55, 31.43, 21.16, 20.82, 19.00, 18.99. Mass spectrometry (ESI-MS, m/z): $[M–2Br]^{2+}$ calcd. for $C_{53}H_{45}N_2O_2PS^{2+}$: 402.1467; found: 402.1489.

CTPP ^{1}H NMR (400 MHz, CD_3OD, ppm): δ 8.69 (d, J = 6.5 Hz, 2 H), 8.14 (d, J = 7.7 Hz, 2 H), 8.06 (d, J = 15.9 Hz, 1 H), 8.00 (d, J = 6.7 Hz, 2 H), 7.97 (d, J = 8.5 Hz, 2 H), 7.90 (t, J = 7.1 Hz, 3 H), 7.85–7.81 (m, 4 H), 7.80–7.74 (m, 8 H), 7.64 (d, J = 8.5 Hz, 2 H), 7.59 (d, J = 3.9 Hz, 1 H), 7.53 (d, J = 3.9 Hz, 1 H), 7.46–7.38 (m, 4 H), 7.28 (t, J = 6.5 Hz, 2 H), 7.08 (d, J = 15.9 Hz, 1 H), 4.53 (t, J = 7.5 Hz, 2 H), 3.55 (td, J = 15.4, 2.8 Hz, 2 H), 2.27–2.20 (m, 2 H), 1.81–1.71 (m, 2 H). ^{13}C NMR (150 MHz, CD_3OD, ppm): δ 153.81, 147.52, 143.53, 140.39, 140.21, 137.88, 135.05, 134.56, 133.75, 133.46, 132.35, 130.30, 127.14, 125.89, 125.12, 123.49, 123.37, 121.06, 120.07, 119.95, 118.46, 117.89, 109.37, 58.98, 31.56, 31.44, 21.19, 20.85, 19.05, 19.03. Mass spectrometry (ESI-MS, m/z): $[M–2Br]^{2+}$ calcd. for $C_{51}H_{43}N_2PS^{2+}$: 373.1437; found: 373.1431.

MTPP ^{1}H NMR (400 MHz, CD_3OD, ppm): δ 8.64 (d, J = 6.7 Hz, 2H), 8.07 (d, J = 15.7 Hz, 1H),

7.99 (d, J = 6.7 Hz, 2H), 7.90 (td, J = 7.1, 1.3 Hz, 3H), 7.83 (t, J = 6.3 Hz, 4H), 7.74–7.80 (m, 8H), 7.56 (d, J = 8.8 Hz, 2H), 7.44 (d, J = 3.9 Hz, 1H), 7.29 (d, J = 3.9 Hz, 1H), 6.97 (d, J = 15.7 Hz, 1H), 6.78 (d, J = 8.9 Hz, 2H), 4.50 (t, J = 7.5 Hz, 2H), 3.55 (td, J = 14.8, 2.4 Hz, 2H), 3.01 (s, 6H), 2.29–2.18 (m, 2H), 1.82–1.69 (m, 2H). ^{13}C NMR (150 MHz, CD_3OD, ppm): δ 154.14, 151.10, 150.96, 143.25, 137.35, 135.21, 135.03, 135.01, 134.63, 133.53, 133.47, 130.29, 130.21, 126.64, 122.85, 121.80, 121.20, 119.12, 118.47, 117.90, 112.11, 58.73, 39.06, 31.49, 31.37, 21.18, 20.83, 19.02, 19.00. Mass spectrometry (ESI-MS, m/z): $[M–2Br]^{2+}$ calcd. for $C_{41}H_{41}N_2PS^{2+}$: 312.1359; found: 312.1355.

Computational Method

The geometrical structures of **TEPP**, **TTPP** and **MTPP** were optimized with hybrid density functional method (B3LYP) in conjugation with 6-31G(d) basis set. Time-dependent DFT (TD-DFT) was adopted to calculate electronic excitation energies and a conductor-like polarizable continuum model (CPCM) was employed in the treatment of solvent effects (water). All theoretical calculations were performed using Gaussian 09 suite of program. GaussView 5.0 was used to generate the contour plot of frontier molecular orbitals (HOMO and LUMO). The SOC levels of **TEPP** and **TTPP** were calculated by Gaussian 09: M062X/def2-SVP SOC: Pysoc.

Cell lines

Human epithelioid cervical carcinoma cell line (HeLa) was supplied by the Institute of Cell Biology (Shanghai, China). Cells were all propagated in T-75 flasks cultured at 37 ℃ under a humidified 5% CO_2 atmosphere in DMEM medium (GIBCO/Invitrogen, Camarillo, CA, USA), which were supplemented with 10% fetal bovine serum (FBS, Biological Industry, Kibbutz Beit Haemek, Israel), 1% penicillin-streptomycin (10,000 U mL-1 penicillin, and 10 mg mL^{-1} streptomycin, Solarbio life science, Beijing, China).

Confocal colocalization for mitochondria

HeLa cells were cultured in the chambers at the density of 5×10^5 mL^{-1} for 24 h. The culture medium was removed, and the cells were rinsed with PBS. HeLa cells were incubated with 5 μM **TEPP**, **TTPP** or **MTPP** in DMEM medium at 37 ℃ for 0.5, 2.5 or 5.5 h. HeLa cells were washed with

PBS and then incubated with 200 nM MTG in DMEM medium at 37 ℃ for 0.5 h. After removing the medium, HeLa cells were washed with PBS for 3 times and imaged by confocal laser scanning microscope. The emission filter: **TEPP**, **TTPP**, **MTPP** 650-750 nm; MTG, 505-550 nm.

Wash-free imaging of TEPP for mitochondria

HeLa cells were cultured in the chambers at the density of 5×10^5 mL^{-1} for 24 h. The culture medium was removed, and the cells were rinsed with PBS. After incubation with 5 μM **TEPP** in DMEM medium at 37 ℃ for 60s, 3 h and 6 h, HeLa cells were directly imaged by confocal laser scanning microscope.

Photostability

The HeLa cells labelled by **TEPP**, MTG and MTR were continuously imaged by confocal laser scanning microscope. **TEPP**, 650-750 nm; MTG, 505-550 nm; MTR, 585-625 nm.

$^1O_2$ detection in aqueous solution

The $^1O_2$ generation was studied using ABDA as an indicator as the absorbance of ABDA decreases upon reaction with $^1O_2$. ABDA (50 μM) was mixed with **TEPP**, **TTPP** and **MTPP** or Rose Bengal (5 μM) respectively in DMSO/PBS (v:v = 1:100) and exposed to white light (λ = 400-800 nm, 10 mW cm^{-2}) irradiation for totally 360 s (time interval: 30 s). The decomposition of ABDA was monitored by the absorbance decrease at 359, 378 and 399 nm. ROS quantum yields of AIEgens were calculated by the equation:

$$\Phi_{AIEgen} = \Phi_{RB} \frac{K_{AIEgen} A_{RB}}{K_{RB} A_{AIEgen}}$$

ROS detection in PBS solution

The ROS generation was studied using H2DCF as an indicator as the fluorescence of H2DCF increases upon reaction with ROS. H2DCF (4 μM) was mixed with **TEPP**, **TTPP** and **MTPP** (10 μM) respectively in DMSO/PBS (v:v = 1:100) and exposed to white light (λ = 400-800 nm, 10 mW cm^{-2}) irradiation for totally 20 s (time interval: 2 s). The reactions were monitored by the fluorescence increase at 523 nm.

$^1O_2$ and OH• detection in PBS solution by EPR

The $^1O_2$ and OH• generation was studied by EPR using TEMP and DMPO as a radical trapping agent. TEMP (0.5 μL) or DMPO (25 mM) was mixed with **TEPP**, **TTPP** and **MTPP** (1 mM) respectively in PBS solution in the darkness or under irradiation for 3 or 10 min. Their EPR spectra were then recorded.

Intracellular ROS detection

The ROS generation in HeLa cells was studied using H2DCF-DA as a ROS indicator. After incubation of HeLa cells with **TEPP** (5 μM) for 2.5 h in the dark, the cells were incubated with H2DCF-DA (10 μM) for 30 min. After incubation, the HeLa cells were washed with PBS and imaged by confocal laser scanning microscope before and after white light irradiation (λ = 400-800 nm, 10 mW cm^{-2}, 10 min).

Cytotoxicity Studies

MTT assays were used to assess the cell viability of Hela cells after incubation under dark condition or white light irradiation. The cells in 96-well plates (NEST Technology) were incubated with **TEPP** or **TTPP** of different concentrations for 30 min in dark. After incubation, one array of plates with cells were exposed to white light irradiation (λ = 400-800 nm, 10 mW cm^{-2}) for 1 h and another array of plates with cells were kept in dark as control. After incubation for 24 h, MTT in PBS solution (10 μL, 5 mg mL^{-1}) was added into each well with 4 h further incubation. Then the SDS solution (100 μL, 1%) was added and the cells were incubated for 8 h. The absorbance of MTT at 595 nm was monitored by the microplate reader (Bio-Rad iMark).

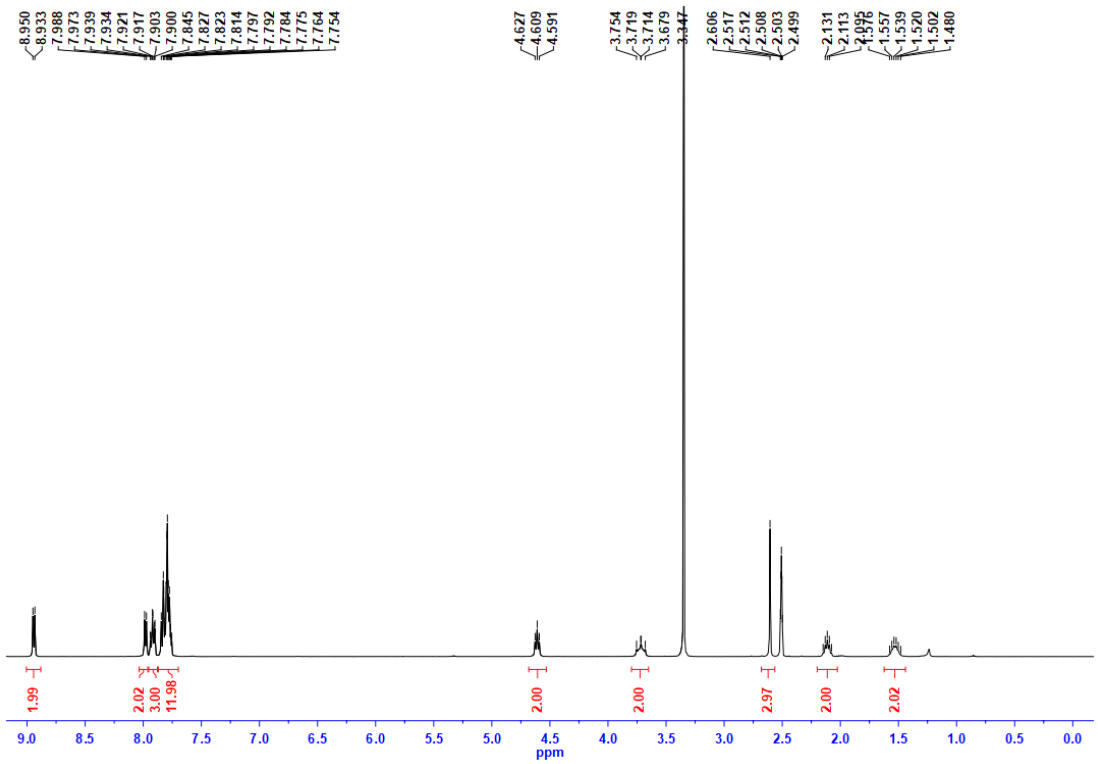

Figure S1. ^{1}H NMR spectrum of compound **2** in DMSO-d_6.

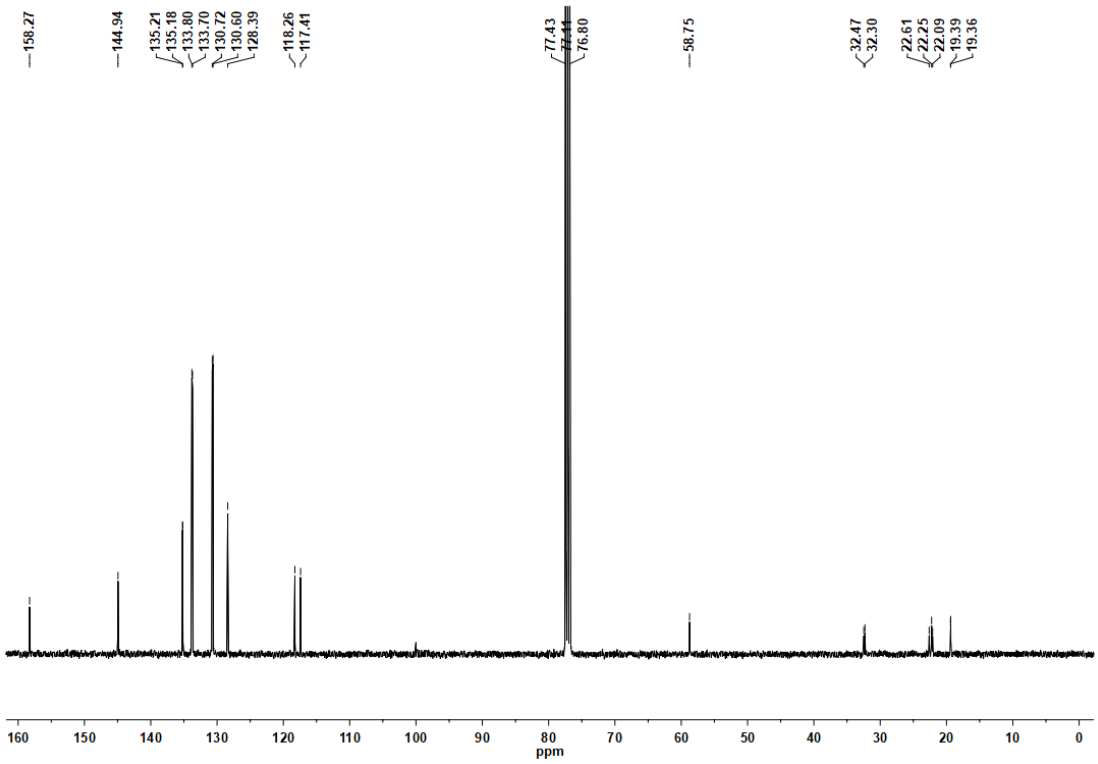

Figure S2. ^{13}C NMR spectrum of compound **2** in $CDCl_3$.

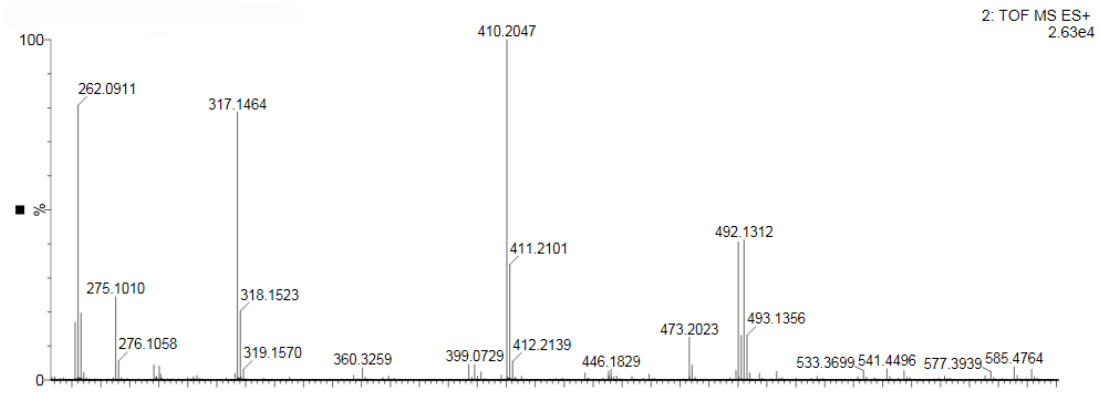

Figure S3. HRMS spectrum of compound **2**.

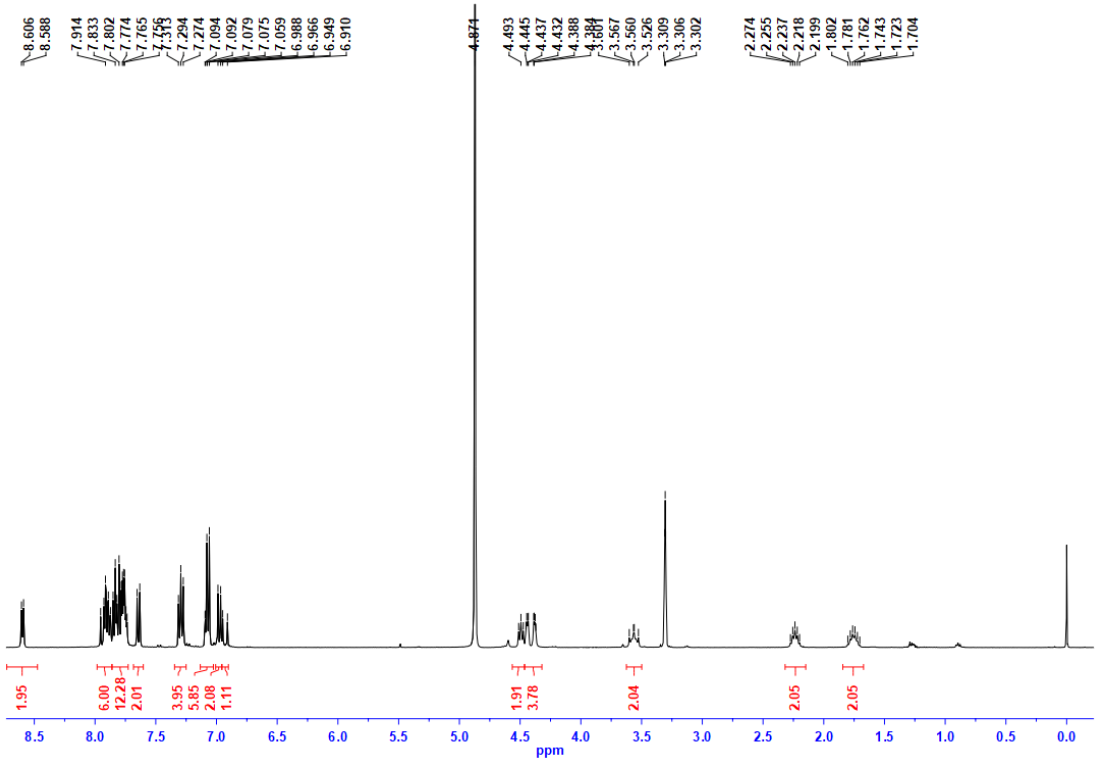

Figure S4. ^{1}H NMR spectrum of **TEPP** in CD_3OD.

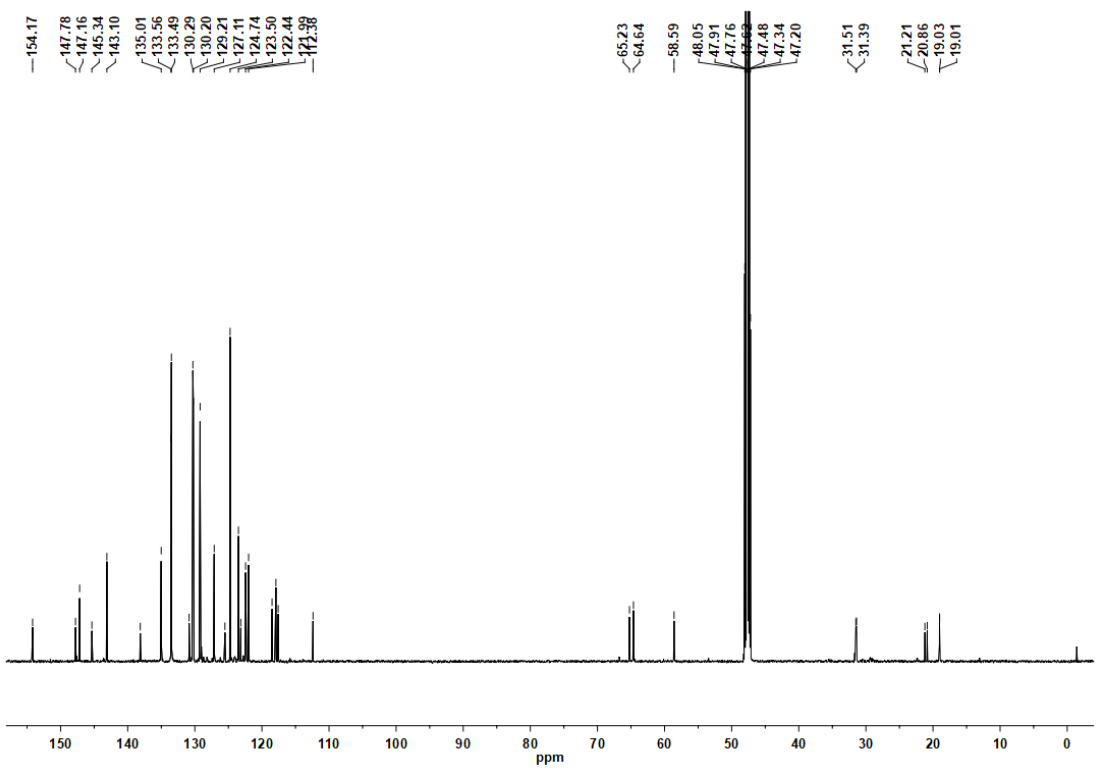

Figure S5. ^{13}C NMR spectrum of **TEPP** in CD_3OD.

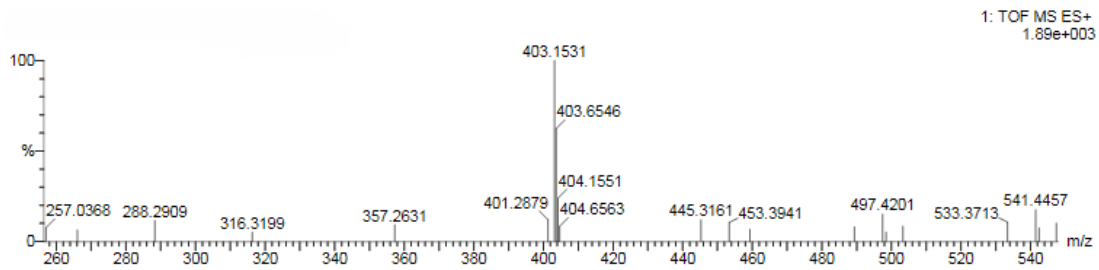

Minimum:				-1.5			
Maximum:		5.0	5.0	50.0			
Mass	Calc. Mass	mDa	PPM	DBE	i-FIT	i-FIT (Norm)	Formula
403.1531	403.1514	1.7	4.2	3.5	23.5	0.0	C18 H33 N2 O P Br

Figure S6. HRMS spectrum of **TEPP**.

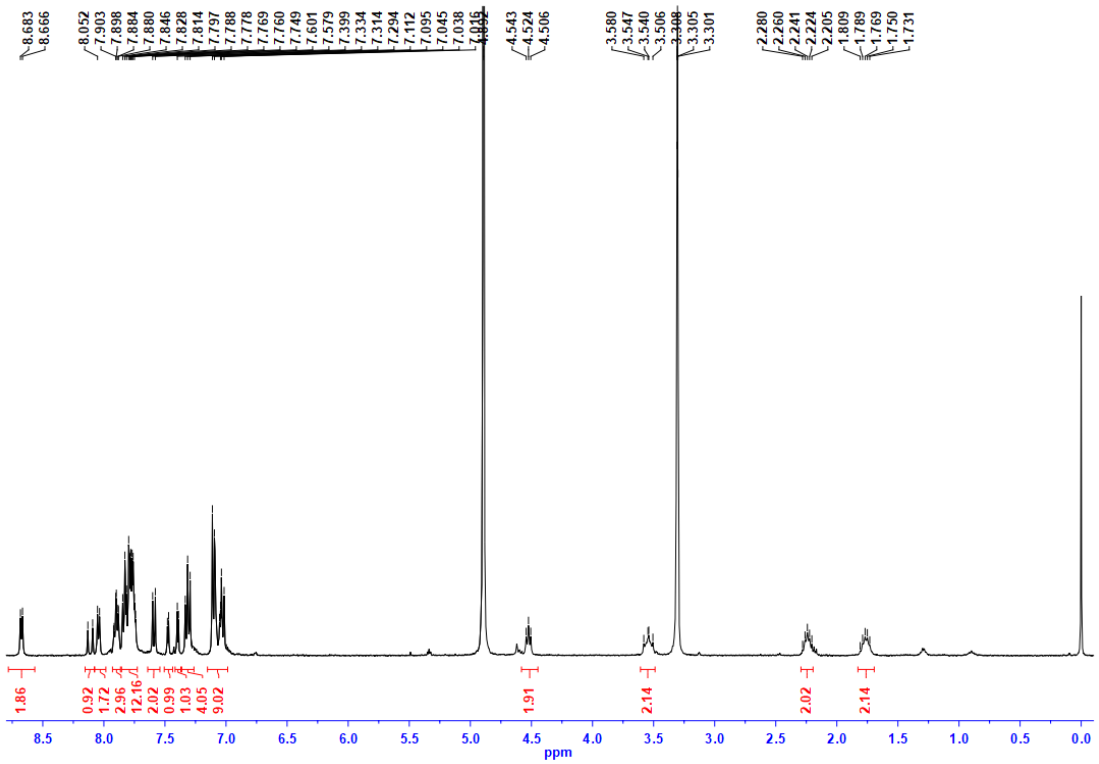

Figure S7. ^{1}H NMR spectrum of **TTPP** in CD_3OD.

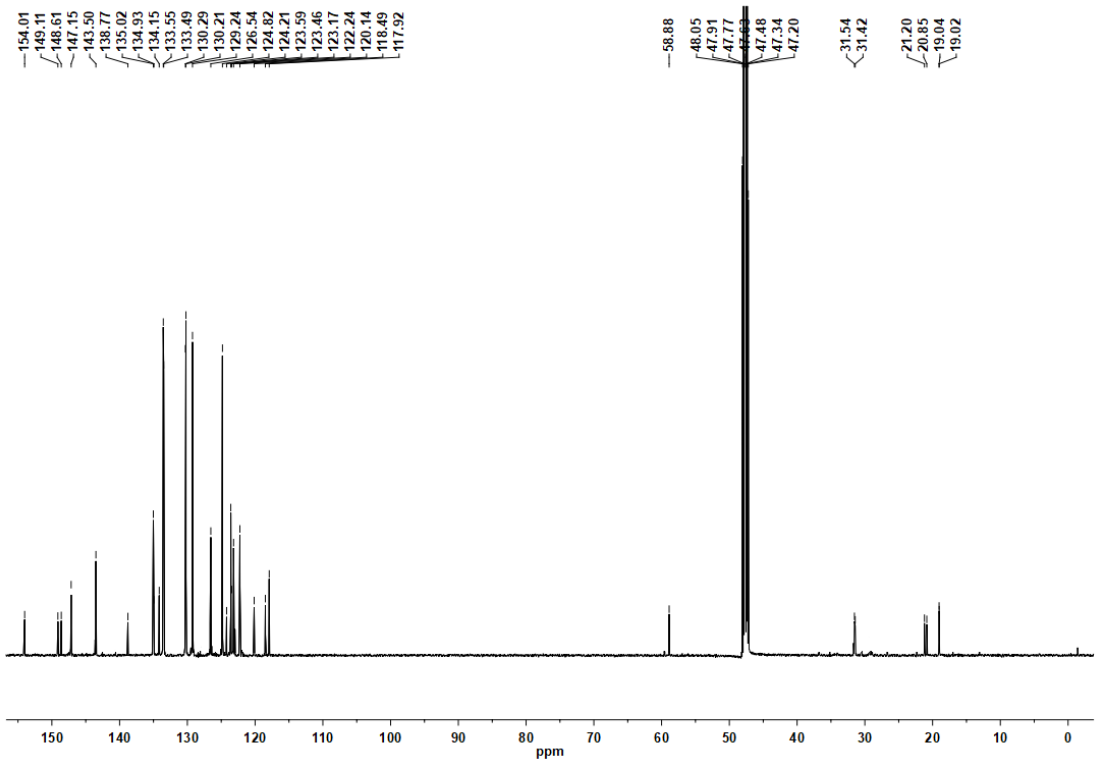

Figure S8. ^{13}C NMR spectrum of **TTPP** in CD_3OD.

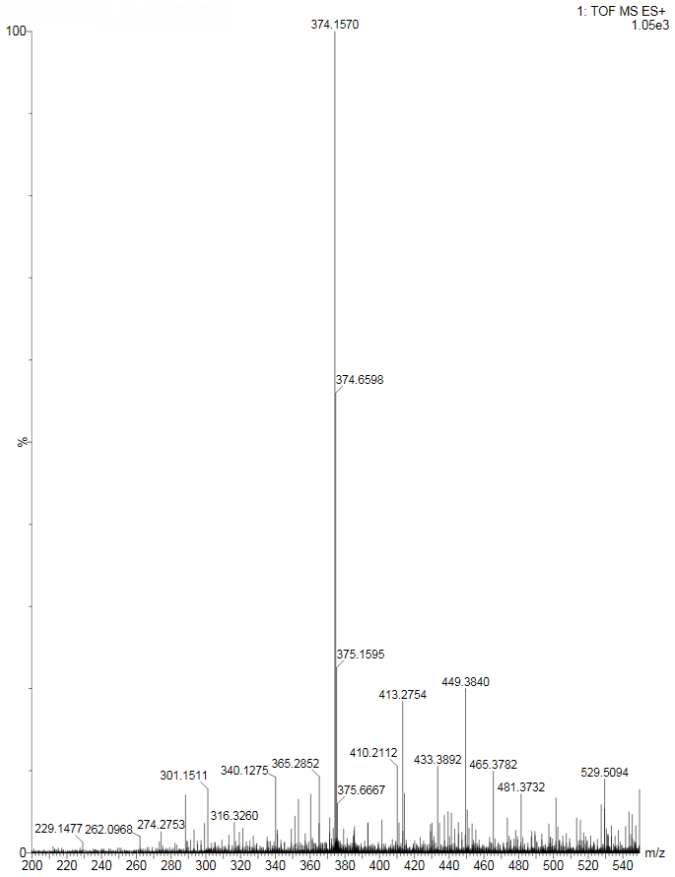

Figure S9. HRMS spectrum of **TTPP**.

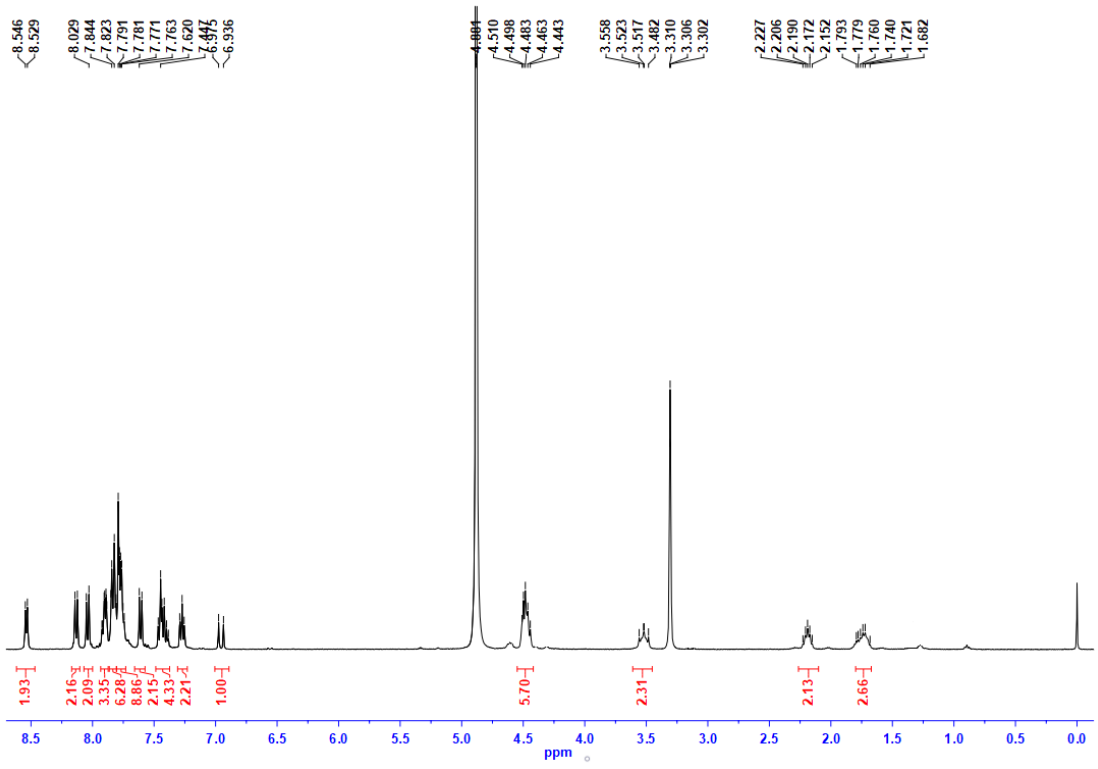

Figure S10. ^{1}H NMR spectrum of **CEPP** in CD_3OD.

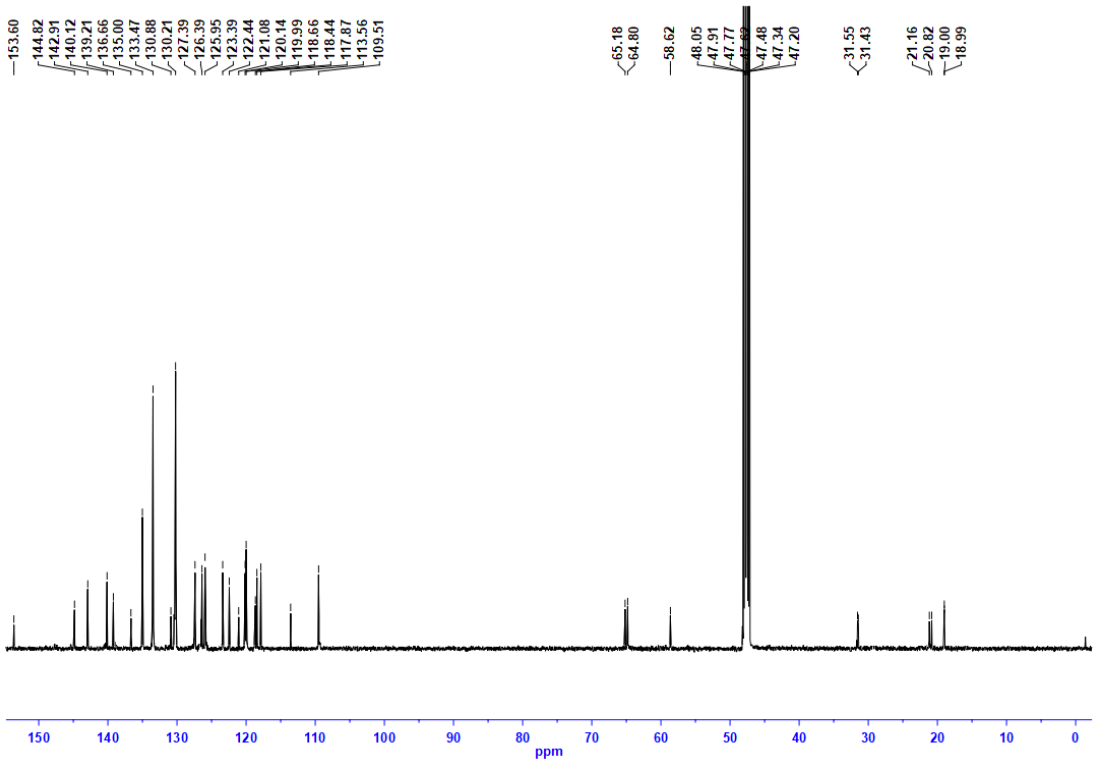

Figure S11. ^{13}C NMR spectrum of **CEPP** in CD_3OD.

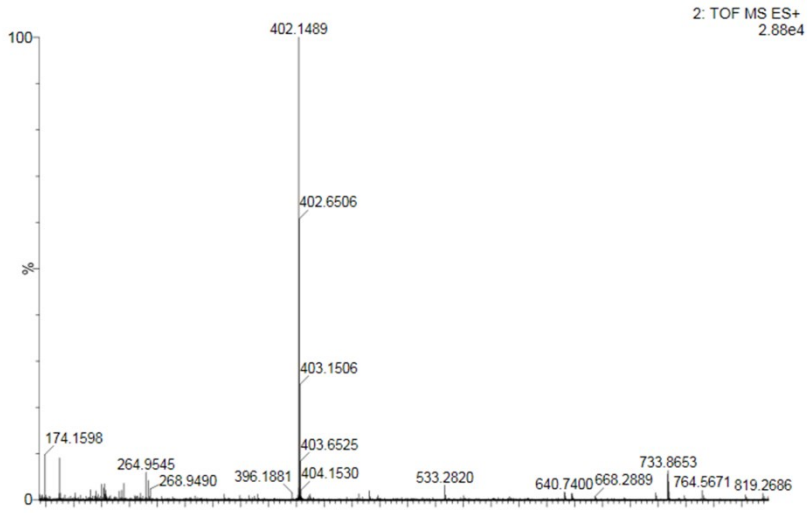

Figure S12. HRMS spectrum of **CEPP**.

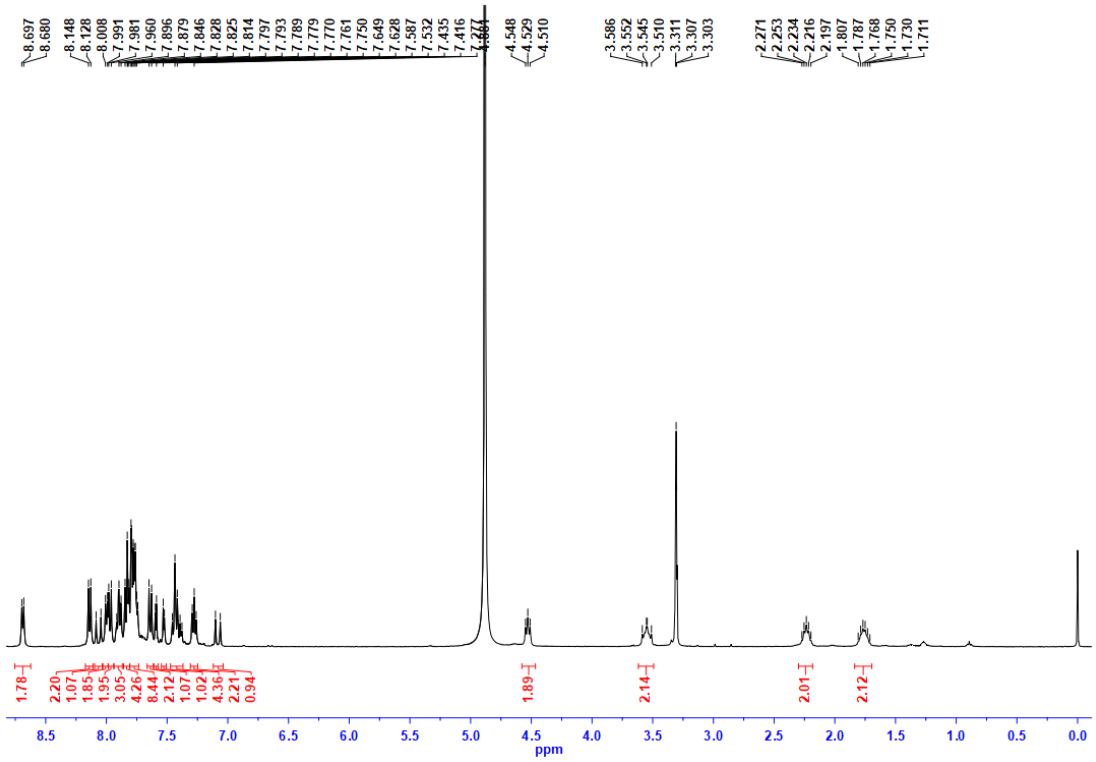

Figure S13. ^{1}H NMR spectrum of **CTPP** in CD_3OD.

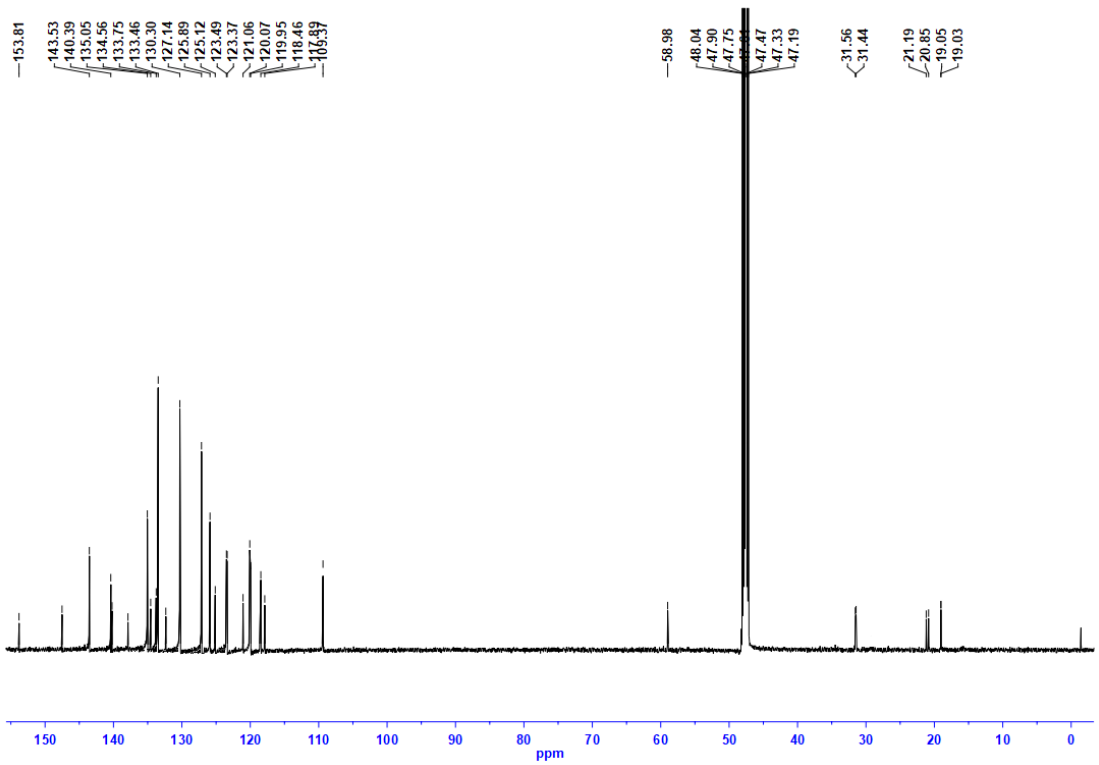

Figure S14. ^{13}C NMR spectrum of **CTPP** in CD_3OD.

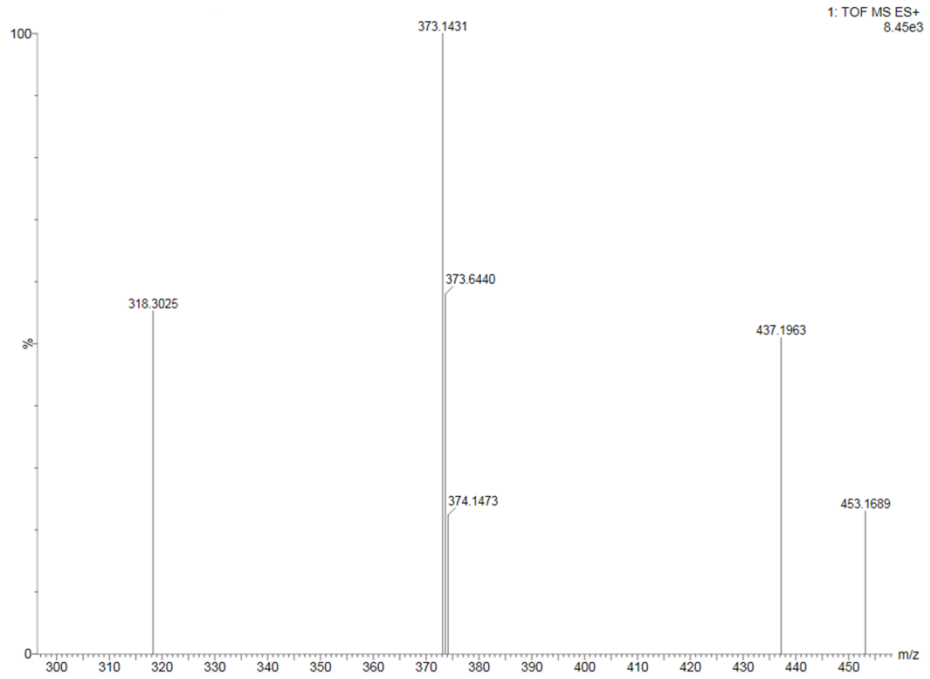

Figure S15. HRMS spectrum of **CTPP**.

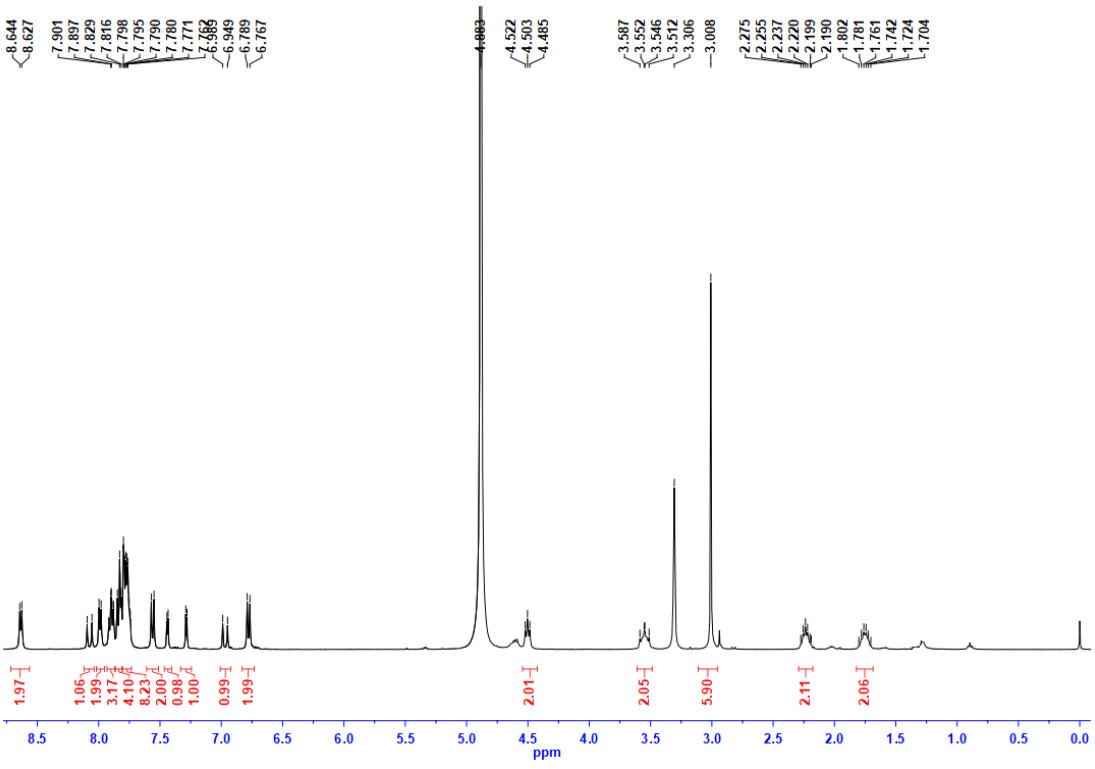

Figure S16. ^{1}H NMR spectrum of **MTPP** in CD_3OD.

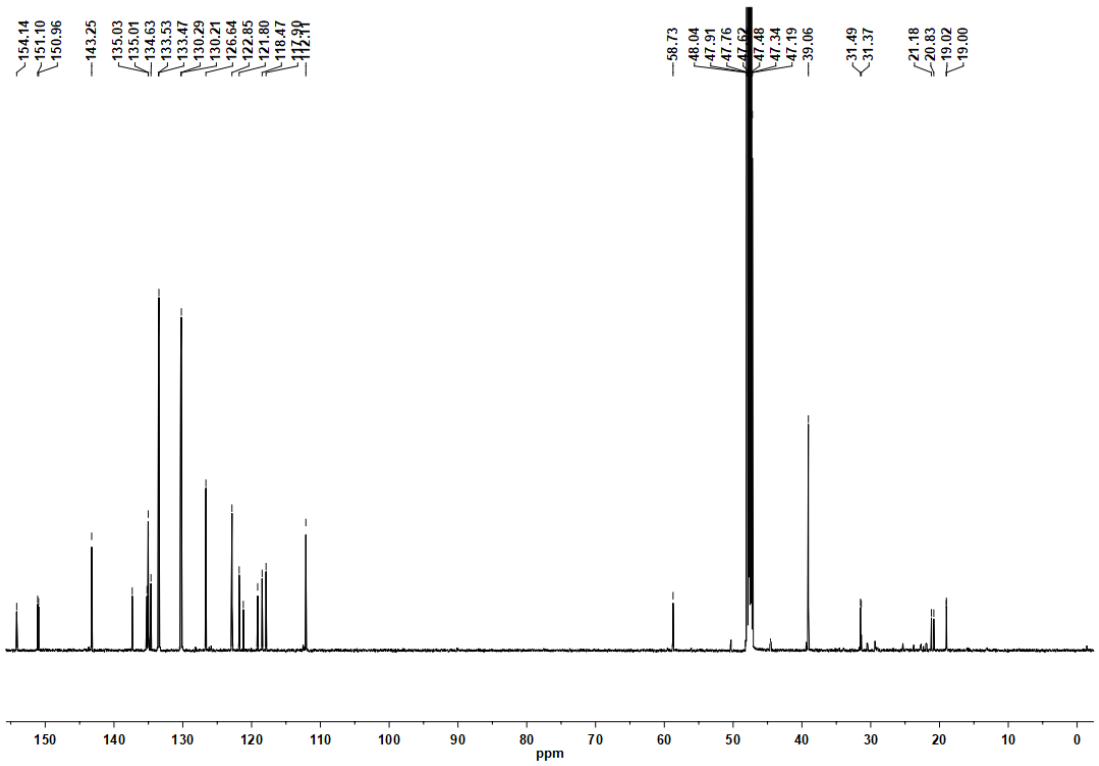

Figure S17. ^{13}C NMR spectrum of **MTPP** in CD_3OD.

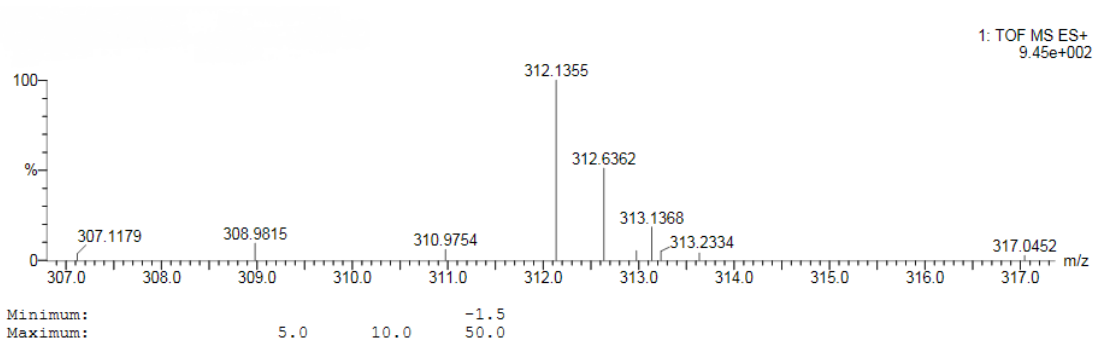

Figure S18. HRMS spectrum of **MTPP**.

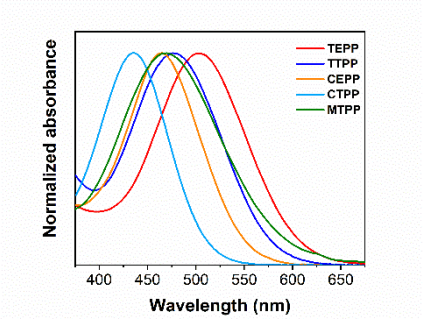

Figure S19. Normalized absorbance spectra of five AIEgens in aqueous solution (Concentration: 10 μM).

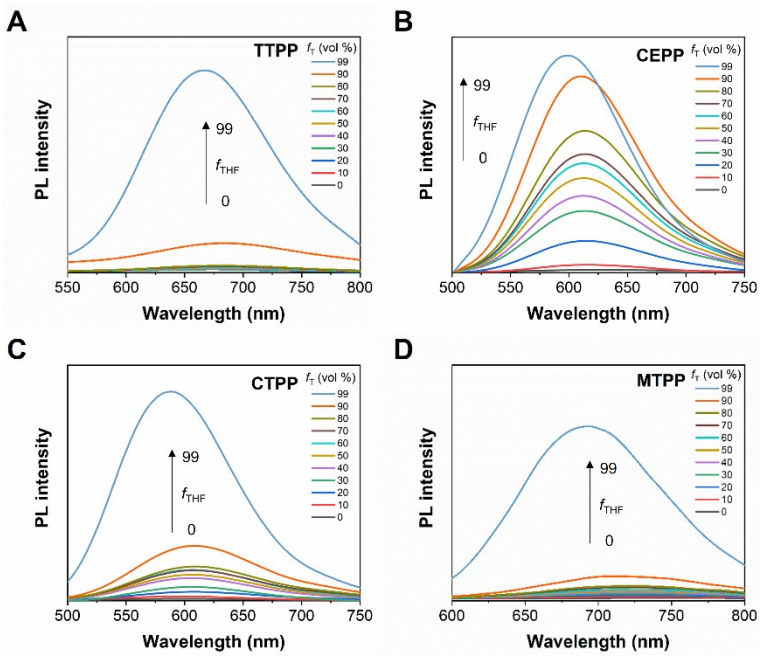

Figure S20. PL intensity spectra of **TTPP** (A), **CEPP** (B), **CTPP** (C) and **MTPP** (D) in THF/H_2O mixture. Concentration: 10 μM.

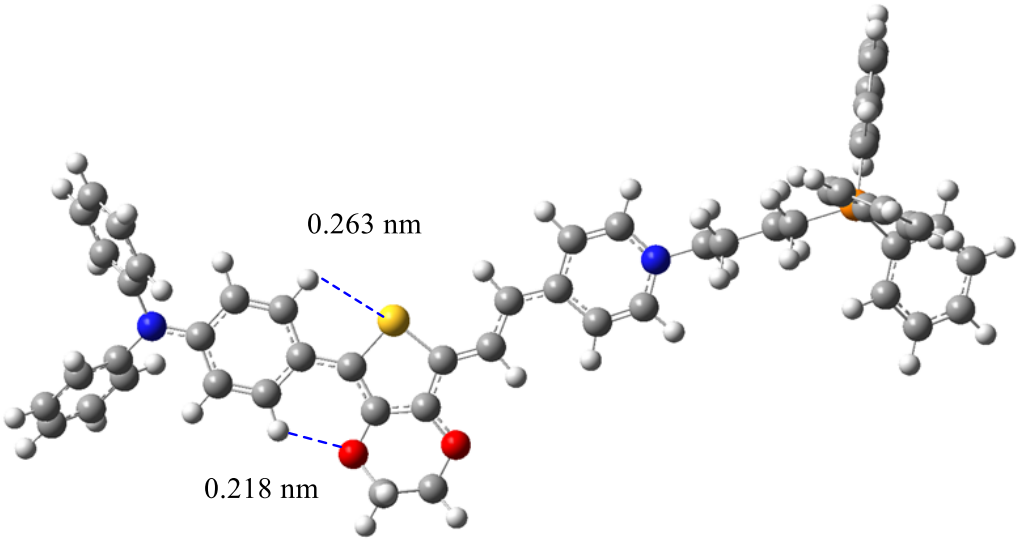

Figure S21. The H···O and H···S interatomic distances of **TEPP** calculated at B3LYP/6-31G(d) level of theory.

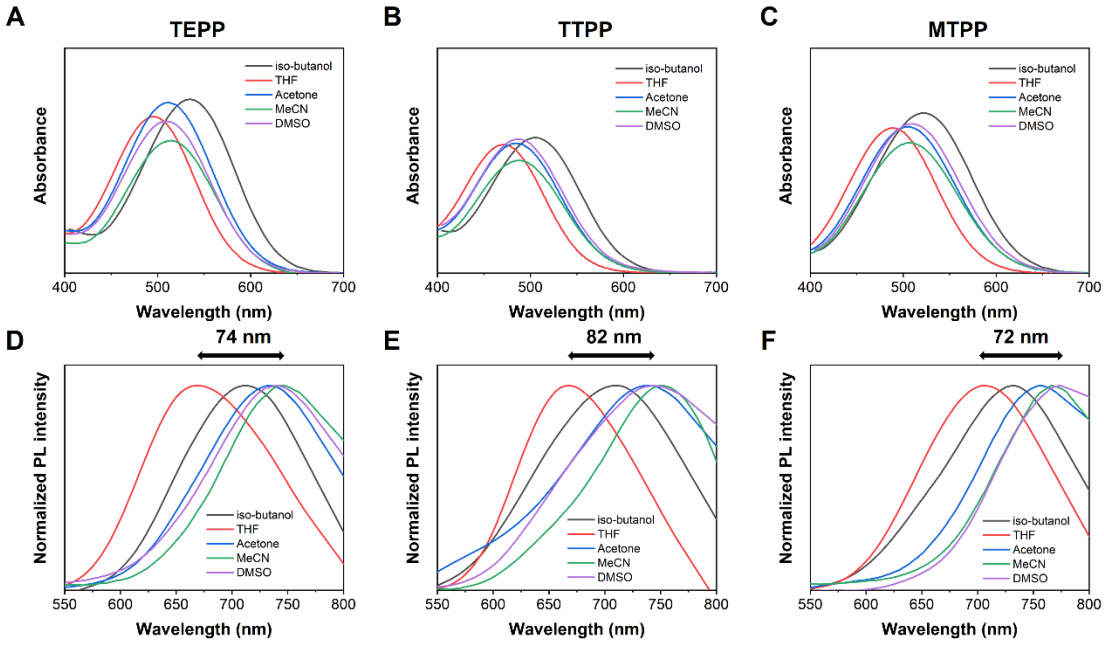

Figure S22. Absorbance spectra and normalized PL intensity spectra of **TEPP**, **TTPP** and **MTPP** in different solvents. Concentration: 10 μM.

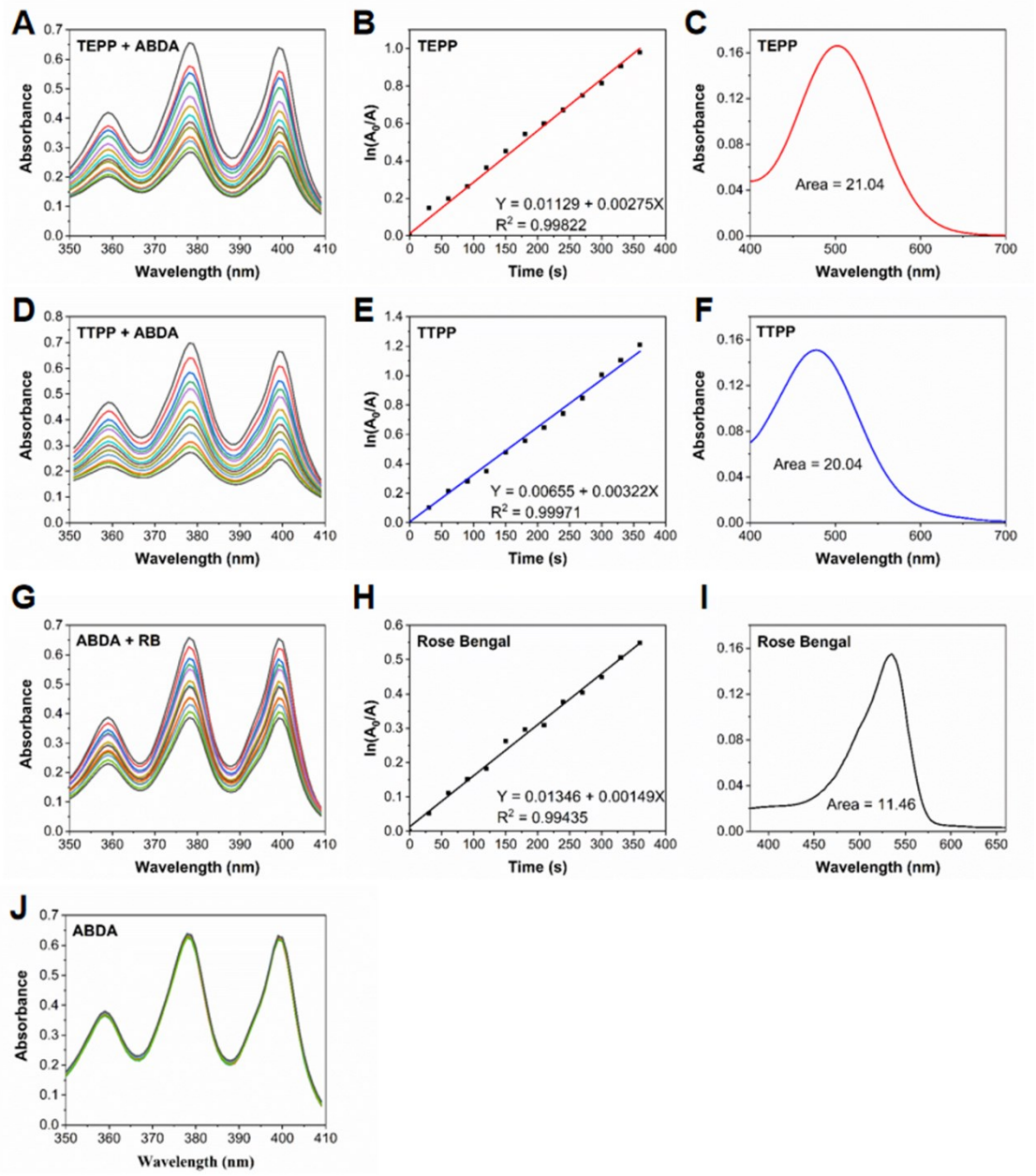

Figure S23. $^1O_2$ quantum yield detection in the aqueous solution upon white light irradiation (λ = 400-800 nm, 10 mW cm^{-2}) for 360 s. UV-vis absorbance of ABDA for the **TEPP** (A), **TTPP** (D), Rose Bengal (G) and control (J) group and their linear fitting (B, E, H) of decomposition of ABDA according to the corresponding UV-vis absorbance. UV-vis absorbance of **TEPP** (C), **TTPP** (F), and RB (I). ABDA (50 μM); **TEPP**, **TTPP** and RB (5 μM).

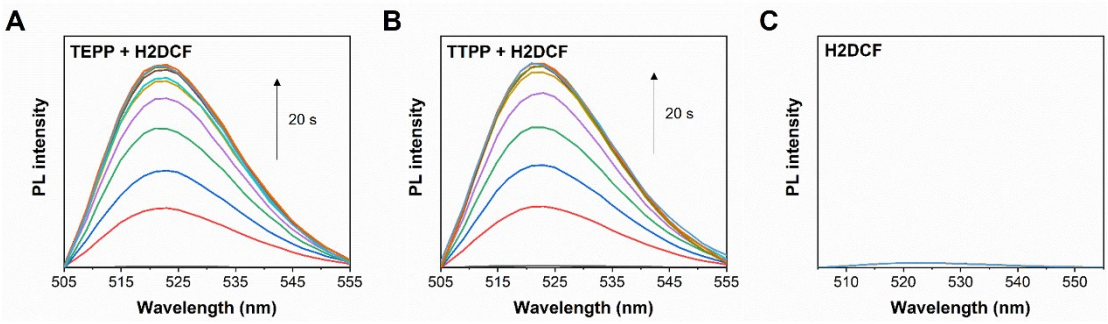

Figure S24. ROS detection in the PBS solution upon white light irradiation (λ = 400-800 nm, 10 mW cm^{-2}) for 20 s. H2DCF (4 μM); **TEPP**, **TTPP** (10 μM).

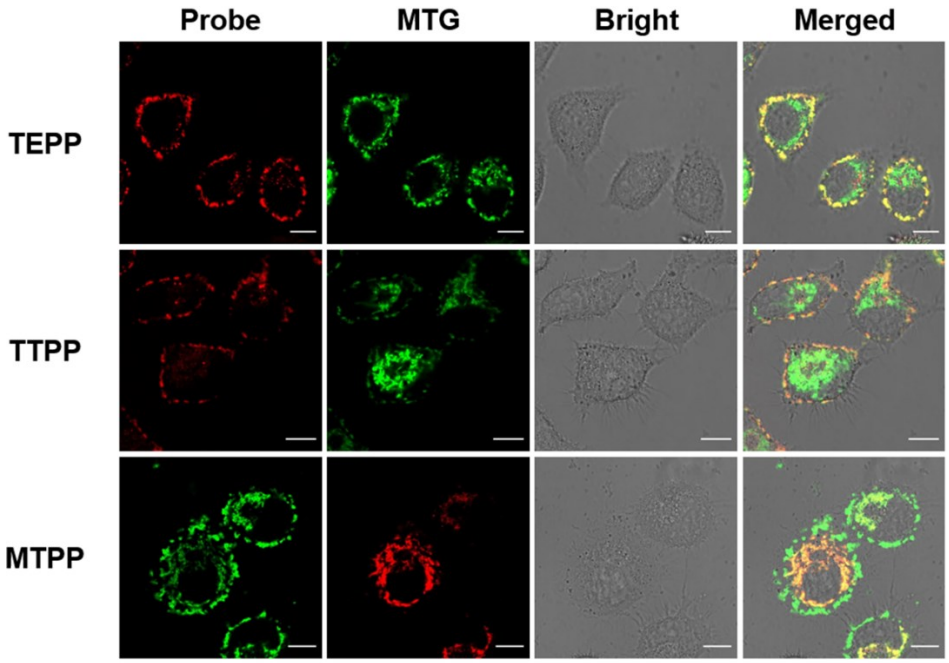

Figure S25. Confocal images of HeLa cells co-stained with AIEgens and MTG for totally 1 h. Concentration: **TEPP**, **TTPP** and **MTPP**, 5 μM; MTG, 200 nM. The emission filter: **TEPP**, **TTPP** **MTPP**, 650-750 nm; MTG, 505-550 nm. The scale bar for all images: 10 μm.

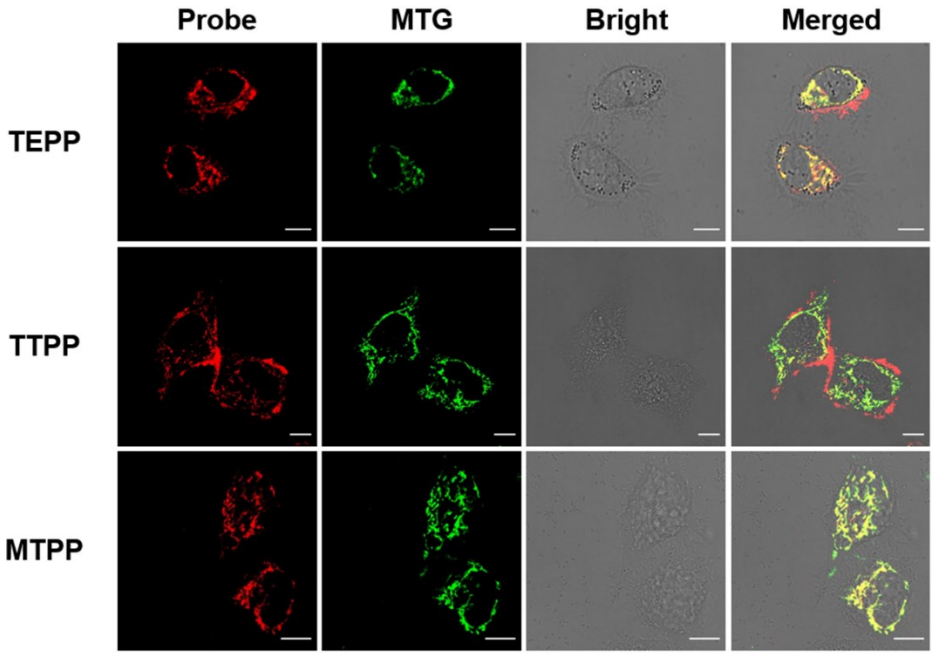

Figure S26. Confocal images of HeLa cells co-stained with AIEgens and MTG for totally 3 h. Concentration: **TEPP**, **TTPP** and **MTPP**, 5 μM; MTG, 200 nM. The emission filter: **TEPP**, **TTPP** **MTPP**, 650-750 nm; MTG, 505-550 nm. The scale bar for all images: 10 μm.

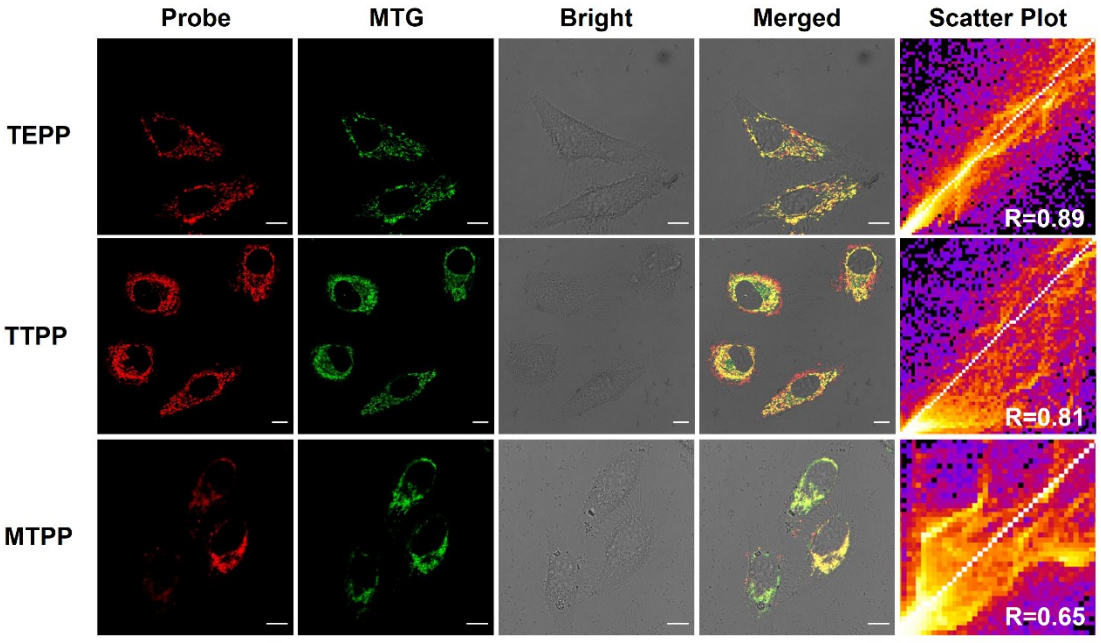

Figure S27. Confocal images and corresponding scatter plot of HeLa cells co-stained with AIEgens and MTG for totally 6 h. Concentration: **TEPP**, **TTPP** and **MTPP**, 5 μM; MTG, 200 nM. The emission filter: **TEPP**, **TTPP** **MTPP**, 650-750 nm; MTG, 505-550 nm. The scale bar for all images: 10 μm.

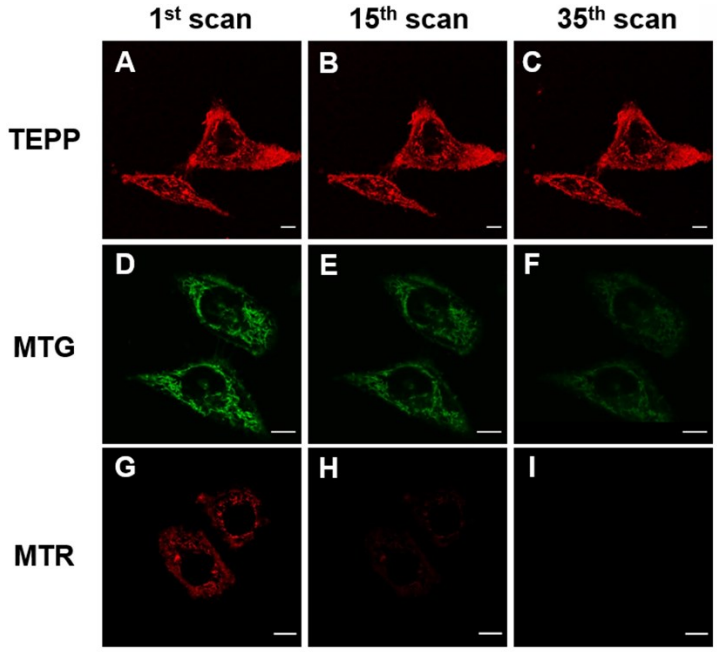

Figure S28. Photostability experiment of **TEPP** on HeLa cells. Confocal images of HeLa cells stained with **TEPP** (A-C), MTG (D-F) and MTR (G-I) after different scanning times. Concentration: **TEPP**, 5 μM; MTG and MTR, 200 nM. The emission filter: **TEPP**, 650-750 nm; MTG, 505-550 nm; MTR, 600-700 nm. The scale bar for all images: 10 μm.

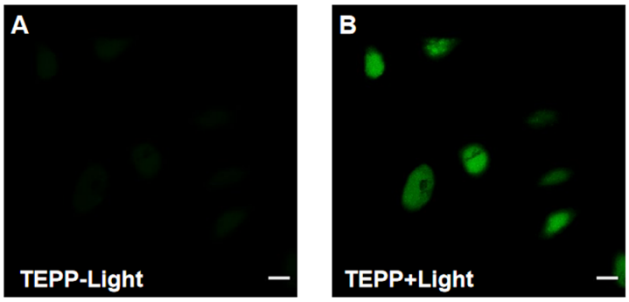

Figure S29. Confocal images of HeLa cells stained with **TEPP** and H2DCF-DA before (A) and after (B) irradiation (λ = 400-800 nm, 10 mW cm^{-2}, 10 min). Concentration: **TEPP**, 5 μM; H2DCF-DA, 10 μM. The emission filter: 505-535 nm. The scale bar for all images: 10 μm.

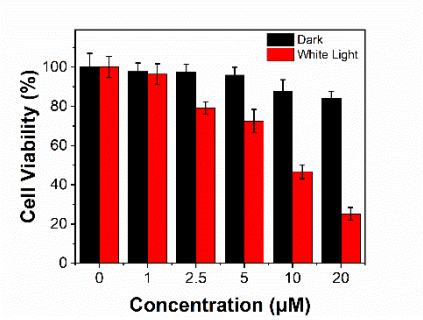

Figure S30. Viability of HeLa cells with different concentrations of **TTPP** and in the absence or presence of white light irradiation (λ = 400-800 nm, 10 mW cm^{-2}, 1 h).

Table S1. Energy levels and energy gaps of HOMO and LUMO for **TEPP**, **TTPP** and **MTPP**.

	TEPP	**TTPP**	**MTPP**
LUMO (eV)	-1.97	-2.02	-5.74
HOMO (eV)	-6.15	-6.24	-9.38
ΔE_g (eV)	4.18	4.22	3.64

Table S2. Dihedral angles (θ_1 and θ_2) for **TEPP**, **TTPP** and **MTPP** calculated at B3LYP/6-31G(d) level of theory.

S_0	θ_1 (º)	Average (º)	θ_2 (º)	Average (º)
TEPP	18.35	18.12	0.61	0.53
	17.88		0.44	
TTPP	17.89	17.63	11.23	11.17
	17.36		11.10	
MTPP	0.03	0.11	2.07	2.05
	0.18		2.03	
S_1	θ_1 (º)	Average (º)	θ_2 (º)	Average (º)
TEPP	62.52	62.57	8.72	9.33
	62.63		9.94	
TTPP	51.99	52.04	9.51	9.59
	52.09		9.66	
MTPP	0.38	0.33	61.39	63.22
	0.27		65.05	

Table S3. Singlet-triplet energy gap and SOC constant of **TEPP** and **TTPP** calculated by Gaussian 09: M062X/def2-SVP, SOC: Pysoc.

	TEPP	**TTPP**
ΔE_{S1T1} (eV)	0.000	0.000
SOC constant (cm^{-1})	0.745	0.794

REFERENCES

1 (a) H. Huang and Y. Tian, *Chem. Commun.*, 2018, **54**, 12198; (b) J. Tang, J. Hua, W. Wu, J. Li, Z. Jin, Y. Long and H. Tian, *Energy Environ. Sci.*, 2010, **3**, 1736; (c) W. H. Liu, I. C. Wu, C. H. Lai, C. H. Lai, P. T. Chou, Y. T. Li, C. L. Chen, Y. Y. Hsu and Y. Chi, *Chem. Commun.*, 2008, 5152; (d) W. Fu, C. Yan, Z. Guo, J. Zhang, H. Zhang, H. Tian and W. H. Zhu, *J. Am. Chem. Soc.*, 2019, **141**, 3171.